Defect recovery and trapping in plastically deformed Au studied by perturbed angular correlations of ^{111}In

Gary S. Collins, Carl Allard, Reinhardt B. Schuhmann, and Christoph Hohenemser
Department of Physics, Clark University, Worcester, Massachusetts 01610
(Received 20 April 1983)

Au samples doped with ^{111}In impurities and heavily deformed at 77 K were studied by perturbed angular correlations after undergoing isochronal annealing up to 500 K. Between 150 and 500 K we detected formation and dissolution of five defect-probe traps characterized by distinctive quadrupole interaction frequencies. Based on previous identifications of four of the traps and arguments that a previously undetected trap forming at 162 K has vacancy character, our experiments suggest trivacancy, divacancy, and monovacancy recoveries at 162, 180, and 240 K, respectively. From the order of the recoveries, we conclude that all three species are present immediately after deformation. For divacancies we observed thermally activated *in situ* transformation between two distinguishable trap configurations. The details of our isochronal annealing curves are well simulated via a kinetic rate model which assumes only first-order processes, and the trapping stages are found to explain most but not all features of stored-energy-release measurements.

I. INTRODUCTION

Microscopic understanding of point-defect recovery in deformed metals is basic to explaining macroscopic failure. Thus, it is of interest to characterize the types of defect species present after deformation, and to study their recovery and accretion into dislocation loops and voids.

The primary experimental methods applied to study this problem have been thermal recovery of resistivity and stored-energy release after deformation at low temperature. These have yielded complex behavior, although, as van den Beukel argued in his review,[1] recovery after deformation is expected to be dominated by defect migration to unsaturable lattice sinks, such as dislocations. One explanation of the observed complexity might be that deformation produces significant populations of several kinds of multidefect clusters, with corresponding overlapping recovery stages that cannot easily be distinguished by these defect nonspecific methods.

To explore this possibility we have used $\gamma\gamma$ perturbed angular correlations (PAC) to "flag" individual defects trapping on ^{111}In impurities in high dilution during recovery of Au after deformation at 77 K. As shown in a recent review,[2] PAC is defect-structure specific: It determines nuclear quadrupole coupling frequencies for defect-associated dopant atoms. We find that significant populations of at least three vacancy-type defects are formed in Au during deformation at 77 K, and that these migrate to sinks and trap in the temperature range $150 < T < 250$ K. The defects in all likelihood are freely migrating monovacancies, divacancies, and trivacancies. Most of the observed trapping behavior can be understood in terms of first-order recoveries of the species to lattice sinks, and does not require significant defect-defect reactions, such as clustering of monovacancies into divacancies during recovery. In this sense our experiments constitute a clearcut confirmation of van der Beukel's expectations.

II. EXPERIMENTAL METHODS

Our samples consisted of 0.125 mm thick polycrystalline foils of 99.998%-purity Au into which ^{111}In had been diffused at 800 °C under an H_2 atmosphere. The ^{111}In concentration was less than 10^{-8} in all cases. While immersed in liquid N_2 the foils were rolled along one direction to the largest possible length increases (ca. 60%) using a jeweler's roller.

PAC measurements were made at 77 K before and after deformation, and after 900 s isochronal annealing steps at selected temperatures up to 500 K. We used a standard, fast-slow coincidence spectrometer with four NaI($T1$) detectors gated on the (171–245)-keV $\gamma\gamma$ cascade of ^{111}Cd (daughter of ^{111}In). Four coincidence spectra, two each at counter angles of 90° and 180°, were combined to obtain the perturbation function, $G_2(t)$. Spectrometer details and data-analysis methods have been described elsewhere.[3]

Figure 1 shows typical spectra measured at 77 K after annealing at various higher temperatures. The spectra were analyzed in terms of one or more quadrupole precession patterns, and interpreted to arise from probe atoms associated with various defect traps. For a randomly directed axial electric field gradient, the perturbation function for nuclear spin $I = \frac{5}{2}$ has the time dependence

$$G_2(t) = \tfrac{1}{5}[1 + \tfrac{13}{7}\cos(\omega_0 t) + \tfrac{10}{7}\cos(2\omega_0 t) + \tfrac{5}{7}\cos(3\omega_0 t)], \quad (1)$$

where $\omega_0 = (3\pi/10)eQV_{zz}/h$ is the coupling frequency of the nuclear quadrupole moment Q in an electric field gradient with principal component V_{zz}. This pattern is illustrated most clearly at the bottom of Fig. 1. For randomly directed, nonaxial electric field gradients $G_2(t)$ also depends on the asymmetry parameter $\eta = (V_{xx} - V_{yy})/V_{zz}$.

The fractional population of probe atoms associated with a particular trap is determined from the amplitude of $G_2(t)$ associated with a particular frequency. Since $G_2(0)$

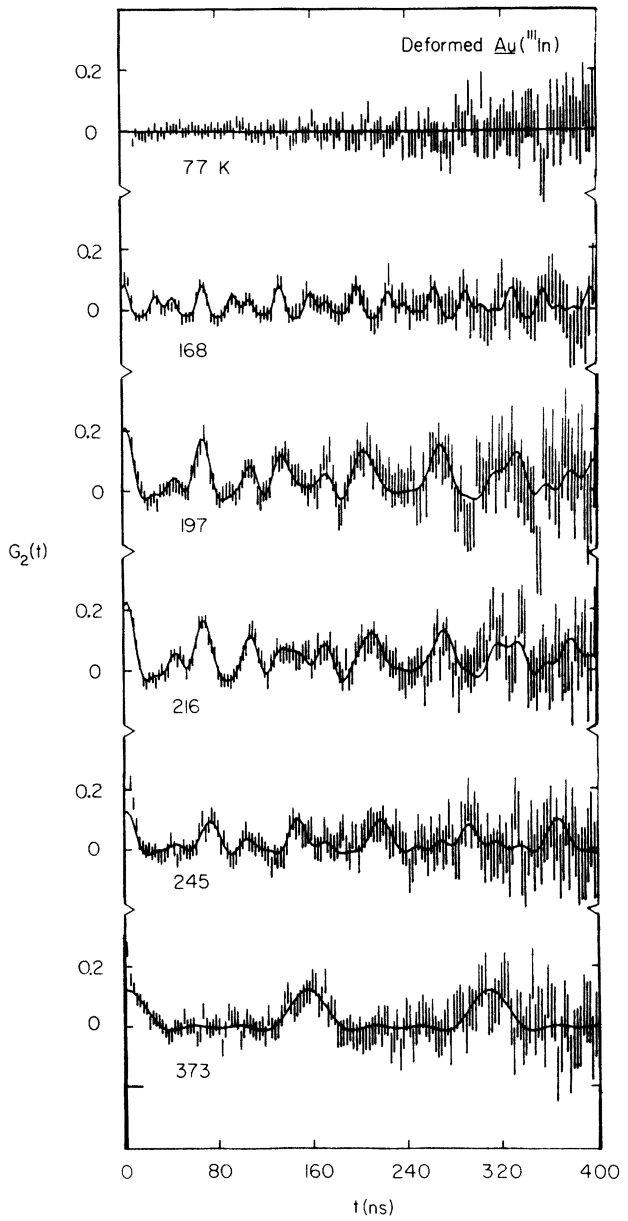

FIG. 1. Perturbation functions $G_2(t)$ for the $\gamma\gamma$ cascade following decay of ^{111}In in Au, after heavy deformation at 77 K and 900 s isochronal anneals at the indicated temperatures. The curves are fits to one or more of five quadrupole precession patterns resulting from formation of defect-probe bound states during recovery.

summed over all sites is normalized to unity, the various precessional signals shown in Fig. 1 correspond to trap populations in the range of 1–20% of the total ^{111}In population.

III. ISOCHRONAL ANNEALING RESULTS

Analysis of spectra measured prior to deformation indicated that $80\pm10\%$ of the ^{111}In probe atoms had cubic environments, as expected for substitutional, defect-free lattice locations. Immediately after deformation at 77 K, and after annealing at 145 and 150 K, no defect trapping was observed down to a detection threshold of 1–2% in site fraction. On the other hand, above 150 K, five trap sites were detected, with average values of ω_0 and η as given in Table I. None of the five patterns identified could be fitted better by allowing for a significant distribution of coupling frequency. Therefore, all five sites are judged to correspond to geometrically well-defined trap geometries. In addition to the sharp frequencies listed in Table I, all spectra also contained distributions of frequencies centered near zero which we believe to be due to distinct defects and/or lattice strain. (These distributed low frequencies have been suppressed in Fig. 1).

Fitted trap fractions are shown as a function of annealing temperature in Fig. 2. Four of the five traps detected (96, 97, 87, and 40 Mrad/s) have been observed by Deicher *et al.*[4] in PAC studies after defects were introduced via ion implantation of ^{111}In, quenching, and irradiation. The fifth, with a frequency of 172 Mrad/s, is observed here for the first time. For convenience, we number the observed trap sites from 1 to 5, starting with the lowest temperature of formation (see Table I).

In their work on quenched and irradiated Au Deicher *et al.* identified the structure of sites 2–5 as follows[4]:

Sites 2 and 3: small defect cluster trapped in two different configurations, based on similar range of appearance of these traps, and roughly equal trapping probabilities after different methods of damaging.

Site 4: monovacancy, based on the ⟨110⟩ direction of the electric field gradient, on its observation after quenching, and observation of substantial trapping after electron irradiation.

Site 5: extended defect, probably a {111} planar faulted loop, based on observation of a variable breakup temperature and the ⟨111⟩ direction of the electric field gradient.

The comparative review of Pleiter and Hohenemser[2] offers additional evidence. Here sites 4 and 5 are shown to be members of two respective classes of defect traps with similar frequencies observed via ^{111}In PAC in several fcc metals, and the class to which site 4 belongs is demonstrated to be the monovacancy via several independent arguments. Finally, in recent, as yet unpublished work[5] Deicher *et al.* have shown rather conclusively that sites 2 and 3 are both divacancy traps. In those experiments[5] Au samples were predoped with sites 2, 3, and 4, and then irradiated at 9 K, a temperature at which only interstitials are mobile. Conversion of sites 2 and 3 into site 4 was observed, presumably via interstitial capture.

In interpreting our results on deformed Au we are, therefore, rather confident in the structure assignments for sites 2–5, as given in Table I. Beyond these assignments our data permit additional interesting conclusions as follows.

(1) Site 1 involves recovery of a new defect. Since site 1 forms well below temperatures at which previously observed and identified traps appear, and has very different quadrupole coupling parameters, it must involve recovery of a third defect species not involved in formation of sites 2–4.

(2) A single migrating species traps to form both sites 2 and 3. We find that sites 2 and 3 are formed at equal temperature to within our experimental accuracy of 1–2 K.

TABLE I. Defect-probe traps forming on ^{111}In during anneals of deformed Au.

Trap	Quadrupole coupling parameters ω_0 (Mrad/s)	η	$\langle hkl \rangle$[a]	$T_{formation}$ (K)	Trap description[b]
1	172 (2)	0.51 (2)		162	trivacancy
2	96 (1)	0.0	not ⟨110⟩	180	divacancy
3	97 (1)	0.44 (2)		180	divacancy
4	87 (1)	0.0	⟨110⟩	240	monovacancy
5	40 (1)	0.0	⟨111⟩	270	extended defect

[a]Electric-field-gradient orientations in single crystals; M. Deicher, E. Recknagel, and Th. Wichert, Radiat. Eff. 54, 155 (1981); M. Deicher, O. Echt, E. Recknagel, and Th. Wichert, in *Nuclear and Electron Resonance Spectroscopies Applied to Materials Science*, edited by E. N. Kaufmann and G. K. Shenoy (North-Holland, Amsterdam, 1981).
[b]The descriptions given are justified in the text, but should not be taken as proven in all cases.

This strongly supports the suggestion of Deicher *et al.*[4] that sites 2 and 3 form via trapping of a single-defect species in two different configurations. Close examination of their trapping curves for irradiated Au, however, indicates a difference of 5—10 K in the formation temperatures of sites 2 and 3, suggesting that two different defects are trapped. Resolution of this apparent discrepancy may involve site 1, which was not seen in irradiated Au, but which has a precession pattern that is easily confused with that of site 2.

(3) Site 2 transforms in situ into site 3 by thermal activation. Examination of Fig. 2 shows that as the site-2 fraction declines near 200 K, site 3 increases in a complementary fashion. However, the sum of the two site fractions (dashed curve in Fig. 2) is observed to remain essentially constant for the entire range over which the sites are stable. These observations strongly suggest that part of the site-2 fraction transforms *in situ* to form site 3, without change in the number of trapped elementary point defects. In this interpretation, site 3 is considered to have a slightly higher binding enthalpy, with transformation proceeding by activated jumping across an enthalpy barrier between the two configurations. Examination of the trapping curves[4] for irradiated Au shows a similar but much less pronounced tendency. In both irradiated Au and our data the transformation is incomplete, i.e., a significant site-2 population persists up to temperatures at which both sites break up. This suggests that the transformation process is substantially affected by small differences in the local environment, and may be promoted in deformed samples by the large lattice strains present.

We conclude that site 1, sites 2 and 3, and site 4 involve trapping of three distinct defect species, and that sites 2 and 3 and site 4 are divacancy and monovacancy traps, respectively. The identity of the species trapping to form site 1 is discussed further below.

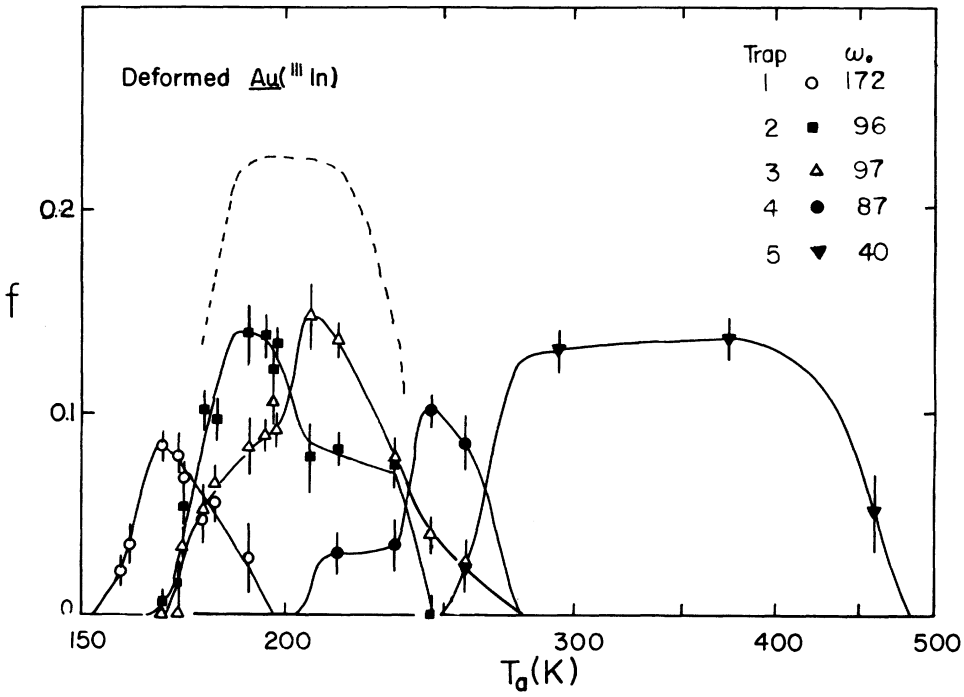

FIG. 2. Fractions f of ^{111}In atoms bound in five defect traps as a function of annealing temperature. The curves are drawn to guide the eye. The dashed curve shows the sum of fractions in sites 2 and 3, which are both observed to start forming at 170 K.

IV. TRAP FORMATION AND DISSOLUTION

In order to relate the evolution of trap populations to a description of defect recovery it is necessary to specify the mechanisms by which the traps form and dissolve. In the simplest case formation of bound states proceeds by trapping of single defects or clusters on the PAC probe atoms, followed at higher temperature by single-step detrapping. Other possible mechanisms involve multiple trapping or accretion of successive defects on the probes, defect-antidefect annihilation at the trap site, and detrapping of only some of the elementary point defects bound to the probe atom. Examination of Fig. 2 suggests that these more complex processes can probably be ignored for several reasons.

(1) Multiple trapping should lead to observation of distinct traps with one, two, or more defects bound to the PAC probe, each with a distinct coupling frequency. In such a process the increase of the population of two-defect traps should be proportional to the fraction of one-defect traps already formed. Such relationships between trap fractions are not evident, although multiple trapping may simply be difficult to observe since detected trap fractions are only of order 10%.

(2) Defect-antidefect annihilation should reduce, but not completely eliminate, trap fractions unless the antidefect concentration and/or capture radius is very large. For traps 1, 4, and 5 no such effect is observed (for sites 2 and 3, as already noted, the explanation of *in situ* trap transformation is plausible for the behavior near 200 K).

(3) Detrapping of some but not all elementary point defects from a probe site should lead to reduction of an existing site fraction to zero, with complementary growth of a new site. No such features are observed.

We assume, therefore, that sites 1–4 form and dissociate by simple trapping and detrapping of three distinct defect species. This assumption is consistent with van der Beukel's conclusion[1] that the lattice sink density is so high that recovery is dominated by migration to sinks. Site 5, attributed to an extended defect trap, could, however, form in a number of alternative ways.[6]

To simulate the trapping behavior of sites 1–4 shown in Fig. 2, and the trap transformation between sites 2 and 3, we employ a kinetic rate model described below. The model is used to estimate migration and binding enthalpies, as well as the initial concentrations of the species observed to recover and trap. The model, however, cannot distinguish whether activation involves recovery of isolated defects or evaporation from agglomerates.

We assume that the concentration, c_n, of a species of defect, d_n, anneals out to lattice sinks independent of the other defect concentrations, via the first-order process $\dot{c}_n = -A_n c_s c_n$, in which c_s is the lattice sink concentration and A_n is the migration rate constant, given by

$$A_n = g_n^M \nu_n^M \exp(-E_n^M/kT) \ . \tag{2}$$

Here E_n^M is the migration enthalpy of d_n, and g_n^M and ν_n^M are corresponding geometrical factors and jump-attempt frequencies. Trapping of defects d_n on defect-free probe atoms, p_0, to form defect-probe bound states, p_{ni}, in the ith configuration, and subsequent detrapping, are described by the reactions $d_n + p_0 \rightleftarrows p_{ni}$. The trapping rate constant T_{ni} depends on A_n, c_n, the dimensionless trapping radius r_n of the defect-free probe for d_n, and on the probability t_{ni} that the defect traps in the ith configuration:

$$T_{ni} = A_n c_n r_n t_{ni} \ . \tag{3}$$

The detrapping rate constant depends on E_n^M, the binding enthalpy E_{ni}^B of the ith configuration, a geometrical factor g_n^D and an attempt frequency ν_n^D:

$$D_{ni} = g_n^D \nu_n^D \exp[-(E_n^M + E_{ni}^B)/kT] \ . \tag{4}$$

In situ transformation between trap configurations i and j involves the reactions $p_{ni} \rightleftarrows p_{nj}$. The transformation rate constant τ_{nij} going from configuration i to configuration j depends on E_n^M, a geometrical factor g_n^τ, an attempt frequency ν_n^τ, the difference of binding enthalpies, $E_{ni}^B - E_{nj}^B$, and the enthalpy barrier between the configurations, $E_{nij}^\tau \equiv E_{nji}^\tau$:

$$\tau_{nij} = g_n^\tau \nu_n^\tau \exp[-(E_n^M + E_{ni}^B - E_{nj}^B + E_{nij}^\tau)/kT] \ . \tag{5}$$

It is easily show that for the reactions described above, the fraction f_0 of defect-free probe atoms p_0 and the fractions f_{ni} of traps p_{ni} evolve according to the set of coupled differential equations

$$\dot{f}_0 = \Sigma_{ni}(-T_{ni} f_0 + D_{ni} f_{ni}) \ , \tag{6a}$$

$$\dot{f}_{ni} = +T_{ni} f_0 - D_{ni} f_{ni} + \Sigma_j(\tau_{nji} f_{nj} - \tau_{nij} f_{ni}) \ , \tag{6b}$$

$$\dot{c}_n = -A_n c_s c_n \ . \tag{6c}$$

For comparison to our experimental results, simulations were made of trapping and recovery by numerical integration of these equations. For simplicity we adopted a constant heating rate $dT/dt = 6.7 \times 10^{-3}$ K/s to describe the isochronal annealing regime, and a constant sink density $c_s = 5 \times 10^{-3}$. We set all geometrical factors $g_n = 12$, the coordination number, and all attempt frequencies $\nu_n = 10^{13}$ s^{-1}. With the use of these values, the trapping curve for the monovacancy (site 4) could be simulated using a migration enthalpy equal to the best published value (Ref. 7), $E_{1V}^M = 0.71(4)$ eV. Other enthalpies and initial defect concentrations were then adjusted to obtain the best overall agreement between the experimental and simulated curves.

Experimental data for sites 1–4 and our best simulation are compared in Figs. 3(a) and 3(b). This shows that major features of the data are reproduced well. In particular, growth of trap populations is modeled well using the assumption of simple trap activation, and the *in situ* transformation between sites 2 and 3 closely follows the experimental pattern.

Also shown in Fig. 3(b) are dotted curves which represent the separate isochronal curves, dc_n/dT, of the three species assumed to be involved in the formation of sites 1–4. Maximum rates of recovery occur at 162, 180, and 240 K, values at which the trapping curves have reached about half their maximum amplitudes.

Parameters used in our best simulation are listed in Table II. To obtain estimates of the initial defect concentrations, $c_n(0)$, one needs to estimate the ^{111}In-defect trap-

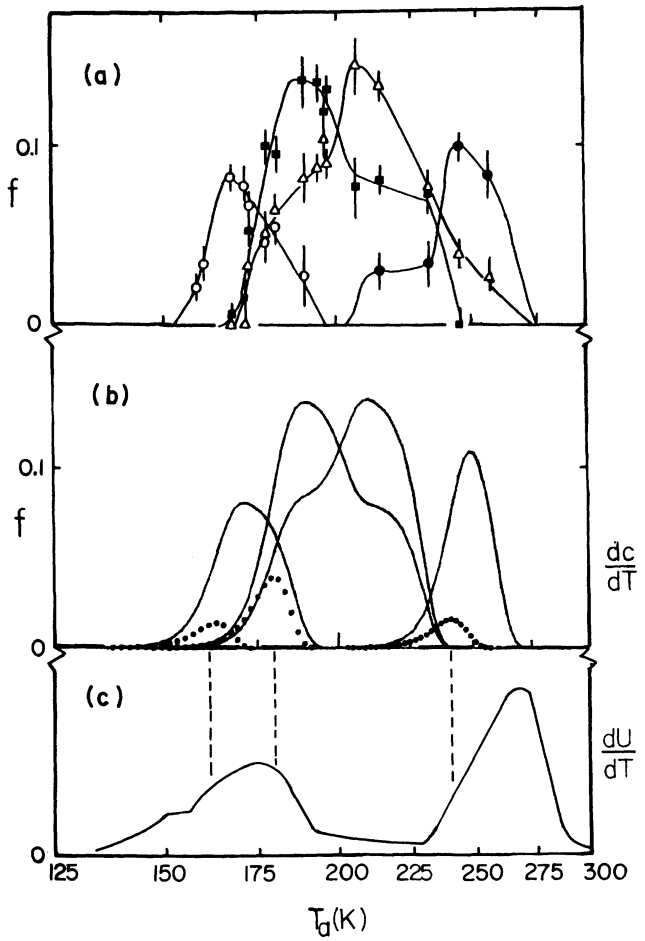

FIG. 3. (a) Experimental trapping behavior for sites 1—4 interpreted to form by trapping of three defect species; (b) simulated trapping behavior (solid curves) and isochronal recovery curves dc/dT of the three species (dotted curves), obtained using a kinetic rate model described in the text; (c) experimental stored-energy-release spectrum dU/dT for heavily deformed Au, redrawn from Ref. 1, with vertical dashed lines indicating the correspondence with simulated recoveries of three defect species.

ping radii. These are expected to range from $r_n = 1$ (negligible long-range elastic interaction) to $r_n = 7$ [the vacancy-interstitial capture radius in Au (Ref. 8)]. For any reasonable choice of r_n, values of $c_n(0)$ are all found to be substantially smaller than the sink density, in accord with our assumption that recovery is dominated by migration to sinks. Binding enthalpies are all found to be of order 0.2 eV. Estimates of migration enthalpies for the two species trapping at 162 and 180 K are 0.475 and 0.525 eV. The true migration enthalpies may of course differ somewhat from these values if the attempt frequencies are much larger or smaller than the 10^{13} s^{-1} values assumed.

Of necessity, the recovery and trapping model we have used here is phenomenological, and involves numerous approximations. In particular, space varying aspects of defect diffusion involving inhomogeneous defect concentrations and lattice strains cannot be properly modeled using a kinetic rate theory. We have shown, however, that a consistent interpretation of experimental trapping curves is obtained on the assumption that defect recovery is dominated by diffusion to lattice sinks.

V. DISCUSSION

A. Comparison to stored-energy release

With confidence gained through simulation of defect trapping and recovery in the case of sites 1—4, we compare our experimental results to stored-energy-release data obtained for Au that has been heavily deformed at 77 K. Results reported by van den Beukel[1] are reproduced in Fig. 3(c) and lead to the following observations.

(1) The recovery of defects 1 and $\frac{2}{3}$ are both observed to fall within the range of the broad stored-energy-release peak extending from 160 to 190 K.

(2) The monovacancy recovery peak at 240 K corresponds to the onset of the broad energy-release peak centered at 260 K, but does not explain it entirely.

(3) The formation of site 5 near 270 K corresponds to the higher-temperature portion of the stored-energy peak centered at 260 K, and together with the monovacancy peak helps explain the latter.

(4) No significant stored-energy recovery is observed near 200 K, the temperature at which site 2 is believed to transform partially into site 3. This gives added confidence for our model of *in situ* transformation between the sites.

Some features of the stored-energy spectrum are not reflected in the PAC data. For example, the small stored-energy peak at 150 K appears to have no counterpart. The possible reasons for this are fairly clear: Not all recovery processes involve point-defect migration which can lead to trapping, and not all recovering species will trap on the ^{111}In probe. It is, nevertheless, remarkable that most of the features of the stored-energy spectrum are paralleled by the more detailed structures of the PAC data.

TABLE II. Kinetic rate model simulation.

Defect and trap parameters		trivacancy site 1	divacancy sites 2 and 3	monovacancy site 4
migration enthalpy	E_n^M (eV)	0.475	0.525	(0.71)[a]
initial concentration	$c_n(0)r_n/c_s$	0.09	0.28	0.15
binding enthalpy	E_n^B (eV)	0.15[b]	0.250/0.255	0.17
transformation enthalpy	E_n^T (eV)		0.17	

[a]Normalization (see text).

[b]Assumes trap dissolution by detrapping; dissolution may proceed by transformation to another trap structure (see text), in which case this parameter has no simple interpretation.

B. The character of site 1

What is the species that recovers at 162 K? We have already argued that site 1 involves trapping of a defect other than the monovacancy or divacancy. This leaves open the possibility of its formation by recovery of an interstitial species or a higher-order vacancy cluster. We argue against interstitial trapping on several grounds, as follows:

(1) While no ^{111}In-interstitial traps have been reported as yet for Au, such traps detected in irradiated Al and Cu have coupling frequencies which are only 10—40 % of the monovacancy trap frequencies,[9,10] i.e., a factor of 5—20 smaller than the site-1 frequency in Au. Since one can expect corresponding traps in different fcc metals to have similar frequencies, as demonstrated for the monovacancy and extended defect classes of traps,[2] it appears highly unlikely that site 1 could be either a single or multiple interstitial trap.

(2) Previously detected ^{111}In-interstitial traps in irradiated Al and Cu have binding enthalpies which are substantially smaller than for site 1.[9,10]

(3) It is not clear that plastic deformation creates significant quantities of interstitials which later can freely migrate and recover upon warming. After deformation at 4 K, most metals do not show large stepwise recovery in stage 1, as observed after irradiation, but instead exhibit only a small and continuous recovery there.[1] Similarly, in ^{111}In PAC experiments[11] and ^{57}Co Mössbauer experiments[12] on deformed Al, interstitial traps that were detected in corresponding irradiation experiments are not observed.

We conclude, therefore, that site 1 in Au is likely to be a multivacancy trap. This assignment finds independent support from the work of Sahu *et al.*[13] The dependence of effective migration enthalpies on quenching temperature in Au could only be interpreted by positing that some other vacancy species more mobile than monovacancies or divacancies is in part responsible for annealing behavior.

The most obvious multivacancy candidate for defect 1 is the trivacancy. This assignment leads to interesting conclusions in the light of other evidence for trivacancy trapping in fcc metals. Only one trivacancy trap has thus far been proposed on the basis of ^{111}In PAC data. This trap forms in ion-implanted,[14] irradiated,[15] and deformed[16] Ni, and has been structurally described as a tetrahedron of vacant lattice sites with an interstitial ^{111}In probe at its center.[14] The electric field gradient at such a site is zero, and hence the site is distinguishable from defect-free probe atoms only in magnetic hosts. In deformed Ni the site forms by simple trapping near 350 K, attains a maximum population as high as 50% of the available probes, and has a binding enthalpy of about 1.1 eV.[17] Molecular statics calculations by Crocker[18] indicate that the relaxed trivacancy is the most stable configuration for pure Cu. Interstitial positions of oversized impurity atoms like In also have been detected directly in channeling measurements on Cu, Al, and Ni by Swanson *et al.*[19—21] These experiments all indicate large site fractions and high thermal stability for the relaxed trap.

We can reconcile the noncubic character and low apparent binding enthalpy of site 1 in Au with the above characteristics if we assume that site 1 is an *unrelaxed trivacancy* trap. In this case, the disappearance of site 1 near 190 K is most likely caused by *in situ* transformation to the (more stable) relaxed, cubic trivacancy configuration. This hypothesis leads to the prediction that channeling experiments should show formation of the tetrahedral interstitial impurity site characteristic of the relaxed trivacancy in Au in the range of 160—190 K. (Such experiments would require use of oversized impurities heavier than Au, e.g., Tl.)

C. Implications for the deformation process

Our data strongly suggest that trivacancies, divacancies, and monovacancies are successively trapped in distinct recoveries at 162, 180, and 240 K in Au that has been heavily deformed at 77 K. From the order in which the recoveries take place, the higher-order vacancy clusters cannot have been formed by clustering of lower-order species during the recoveries, and must be present immediately after deformation. This phenomenology can be understood from what is generally known about point-defect production in deformed metals. Most models of deformation in fcc metals[1,22] involve nonconservative dragging of jogs on dislocations and dislocation interactions which leave behind strings of interstitials or vacancies. During deformation at 77 K the interstitials move rapidly and either agglomerate in loops or disperse to sinks, with some annihilating at immobile vacancies. The annihilations, in effect, cut the vacancy strings at random locations, leaving behind vacancy debris consisting of single vacancies and small clusters. The relative concentrations of vacancy species thus formed should depend on the importance of competing processes: for example, the relative numbers of vacancies and interstitials produced, and the efficiency of the vacancy strings *vis-a-vis* the dislocations for absorbing the interstitial flux. In subsequent anneals the more mobile small clusters then recover and trap, leaving behind a residue of larger, immobile clusters which may form the nuclei for extended vacancy agglomerates.

VI. SUMMARY AND CONCLUSIONS

Using the defect-specific PAC technique, we detected recovery and trapping of three defect species in Au over the range of $150 < T < 250$ K, after heavy deformation at 77 K. Building on previous vacancy identifications of two of the species, we argued that the third species is the trivacancy. The measurements indicate that the trivacancy recovers at 162 K, the divacancy at 180 K, and the monovacancy at 240 K.

From the order of the recoveries, all three species must already be present after deformation at 77 K. Because the concentrations annealing out are found to be comparable, they lead to a complex spectrum of recoveries when studied by defect nonspecific techniques, as van den Beukel maintained.[1] The PAC technique was found capable of explaining much of the structure of stored-energy-release curves through its ability to trace the separate recoveries of the species.

A novel feature of our measurements involves the direct

observation of thermally activated *in situ* transformation between two divacancy trap structures. Such transformation does not appear to have been previously observed, and surprisingly, is weak or absent for the same two traps in irradiated Au. It was suggested that the large strain fields present in the deformed samples may promote this process. Our hypothesis that site 1 is an unrelaxed trivacancy trap which later converts to the cubic, relaxed configuration offers a second potential illustration of the same phenomenon.

Perhaps the most interesting question raised by this work is how several mobile vacancy species, including the trivacancy, arise during deformation. One model for this comes from the string cutting mechanism for cluster formation we have described. Since the model can be equally applied to other deformed metals, it suggests that substantial concentrations of multivacancy defects are a general consequence of deformation. Further work is needed before this can be conclusively accepted.

ACKNOWLEDGMENT

This material is based upon work supported by the National Science Foundation under Grant No. DMR 81-08307.

[1]A. van den Beukel, in *Vacancies and Interstitials in Metals,* edited by A. Seeger, D. Schumacher, W. Schilling, and J. Diehl (North-Holland, Amsterdam, 1970), p. 427.

[2]F. Pleiter and C. Hohenemser, Phys. Rev. B 25, 106 (1982).

[3]A. R. Arends, C. Hohenemser, F. Pleiter, H. de Waard, L. Chow, and R. M. Suter, Hyperfine Interact. 8, 191 (1980).

[4]M. Deicher, E. Recknagel, and Th. Wichert, Radiat. Eff. 54, 155 (1981).

[5]M. Deicher, R. Minde, E. Recknagel, and Th. Wichert, Univ. Konstanz, Jahresbericht 1980 (unpublished), p. 22; M. Deicher, R. Minde, and Th. Wichert, Jahresbericht 1981 (unpublished), p. 21; R. Minde, M. Deicher, and Th. Wichert, Jahresbericht 1982 (unpublished), p. 32.

[6]M. Deicher, O. Echt, E. Recknagel, and Th. Wichert, Hyperfine Interact. 10, 667 (1981).

[7]K. Sonnenberg and U. Dedek, Radiat. Eff. 61, 175 (1982); see also Refs. 2 and 4.

[8]M. W. Thompson, *Defects and Radiation Damage in Metals* (Cambridge, London, 1969), pp. 264, 279.

[9]H. Rinneberg, W. Semmler, and G. Antesberger, Phys. Lett. 66A, 57 (1978); R. Butt, W. Semmler, and H. G. Müller, *Proceedings of the Fifth Yamada Conference on Lattice Defects and Defect Interactions,* edited by J. Takamura, M. Doyama, and M. Kiritani (University of Tokyo, 1982). (The coupling frequency of the monovacancy trap for Al has not been measured, but is estimated to be 230 Mrad/s in Ref. 2).

[10]M. Deicher, O. Echt, E. Recknagel, and Th. Wichert, in *Nuclear and Electron Resonance Spectroscopies Applied to Materials Science,* edited by E. N. Kaufmann and G. K. Shenoy (North-Holland, Amsterdam, 1981), p. 435. See also M. Deicher, R. Minde, E. Recknagel, and Th. Wichert, Univ. Konstanz, Jahresbericht 1980 (unpublished), p. 15; Jahresbericht 1981 (unpublished).

[11]H. G. Müller, Z. Phys. B 47, 119 (1982).

[12]K. Sassa, W. Petry, and G. Vogl, Philos. Mag. A (in press).

[13]R. P. Sahu, K. C. Jain, and R. W. Siegel, J. Nucl. Mater. 69-70, 264 (1978).

[14]C. Hohenemser, A. R. Arends, H. de Waard, H. G. Devare, F. Pleiter, and S. A. Drentje, Hyperfine Interact. 3, 297 (1977).

[15]R. M. Suter, M. Haoui, and C. Hohenemser, Hyperfine Interact. 4, 711 (1978).

[16]G. S. Collins, G. P. Stern, and C. Hohenemser, Phys. Lett. 84A, 239 (1981).

[17]G. S. Collins and R. B. Schuhmann, Hyperfine Interact. (in press).

[18]A. G. Crocker, M. Doneghan, and K. W. Ingle, Philos. Mag. A 41, 21 (1980).

[19]L. M. Howe and M. L. Swanson, in *Proceedings of the Fifth Yamana Conference on Lattice Defects and Defect Interactions,* edited by J. Takamura, M. Doyama, and M. Kiritani (University of Tokyo, Tokyo, 1982), p. 53.

[20]M. L. Swanson, L. M. Howe, J. A. Moore, and A. F. Quenneville, J. Phys. F 11, L185 (1981); M. L. Swanson, L. M. Howe, T. E. Jackson, and J. A. Moore, Nucl. Instrum. Methods 194, 165 (1982).

[21]M. L. Swanson *et al.* (unpublished).

[22]J. I. Takamura, in *Physical Metallurgy,* edited by R. W. Cahn (North-Holland, Amsterdam, 1970), p. 857.